SUPPLEMENTAL MATERIAL

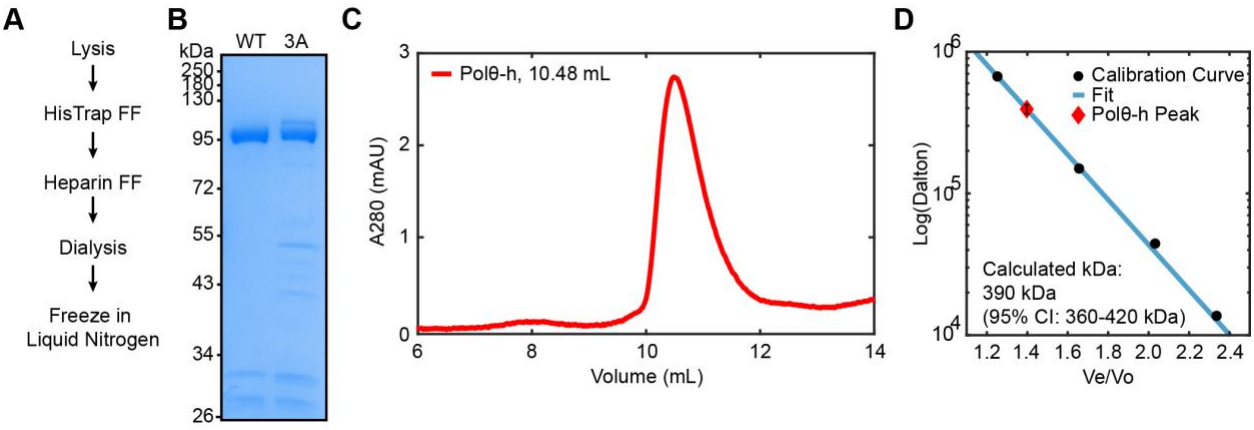

Figure S1: Polθ-h purification and analysis. (A) Schematic of the Polθ-h purification protocol. **(B)** SDS-PAGE gel of purified WT and 3A Polθ-h. The expected molecular weight is 99 kDa. **(C)** Superdex-200 chromatogram of recombinant homotetrameric Polθ-h. **(D)** Calculated molecular weight compared to a molecular weight standard (Sigma-Aldrich, 69385). Error bar within the diamond denotes a 95% confidence interval (CI).

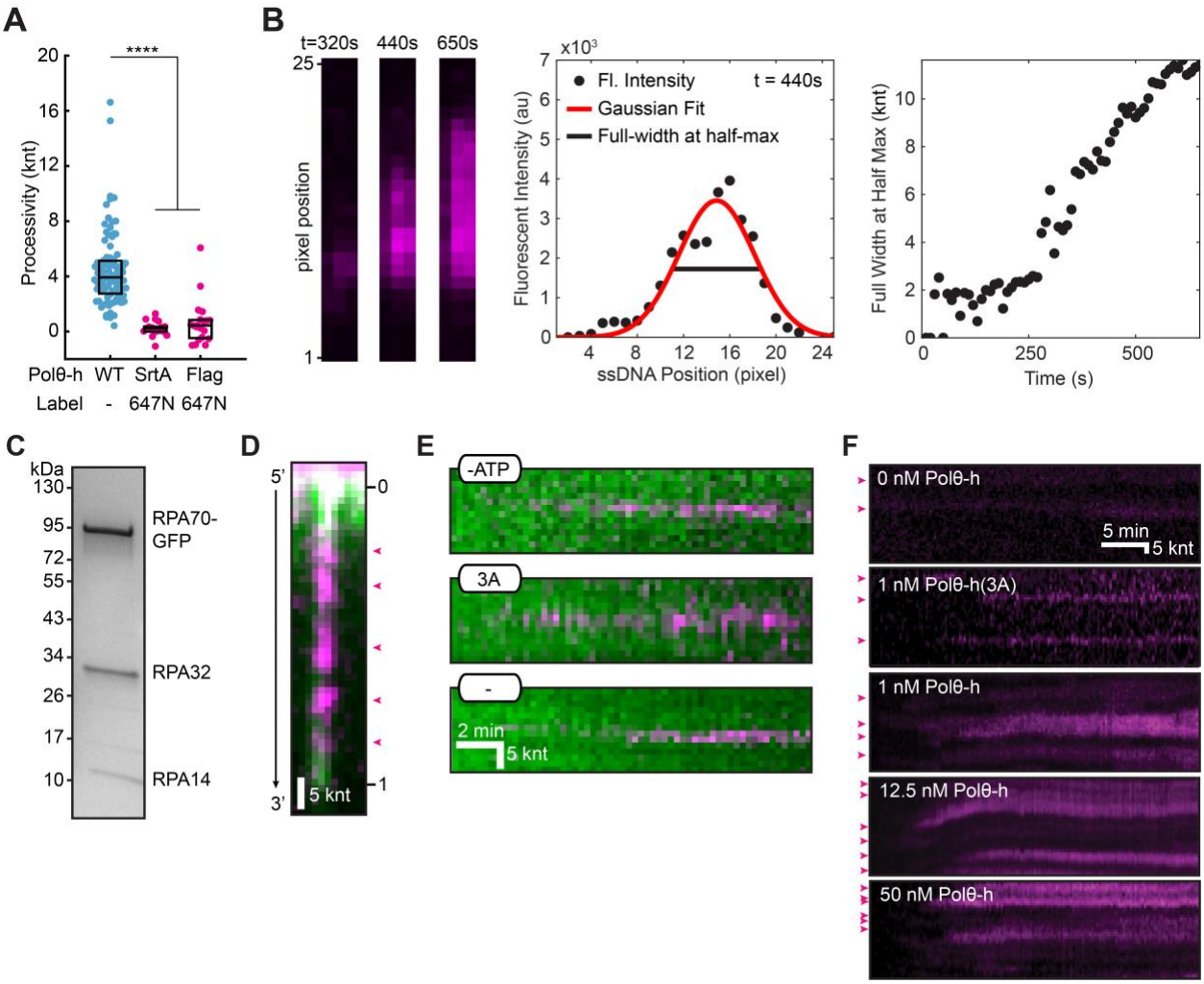

Figure S2: Fluorescent analysis of Polθ-h variants and their translocation activities. (A) We attempted to fluorescently label Polθ-h via sortase-mediated transpeptidation of the N-terminus or the linker region (C-terminus). N-terminal labeled Polθ-h was completely inactive. C-terminal Sortase (SrtA) or Flag epitope labeled Polθ-h constructs showed decreased processivity relative to WT Polθ-h on RPA coated ssDNA. Therefore, we focused on the WT Polθ-h for this study. Box displays median and IQR. **(B)** Summary of how Polθ-h translocation activity was analyzed via fluorescent proxies. Left: individual time points of fluorescent oligonucleotides hybridizing to the DNA. Middle: Gaussian fit of the resulting fluorescent signal. Right: A plot of the full width at half max of this fit as a function of time. **(C)** SDS-PAGE gel of recombinantly purified RPA-GFP. Expected molecular weights are 97, 29, and 14 kDa. **(D)** Analysis of Polθ-h RPA removal locations on single-tethered ssDNA curtains. Due to heterogeneity in their length, ssDNAs are normalized to unit length in a 5' to 3' direction. Magenta arrows show oligonucleotide foci that denote RPA removal activity. **(E)** Kymographs of Polθ-h-mediated RPA-GFP removal controls. ATP and hydrolysis activity are both required to see robust RPA removal. **(F)** Kymographs of concentration dependent Polθ-h oligonucleotide foci (magenta arrows) on RPA-GFP ssDNA curtains.

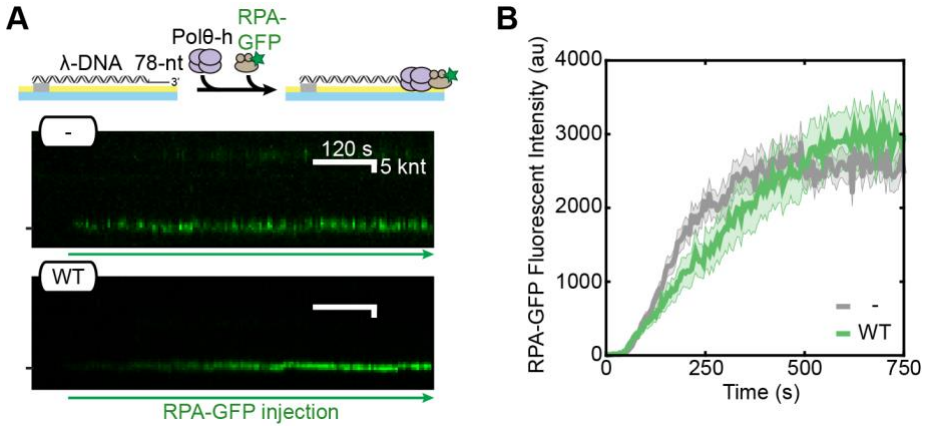

Figure S3: Polθ-h is not a processive dsDNA helicase. (A) Cartoon and kymographs of pre-resected helicase assay substrate in the presence and absence of Polθ-h WT. **(B)** RPA-GFP foci fluorescent intensity over time. WT (N=27) and without Polθ-h (-) (N=43).

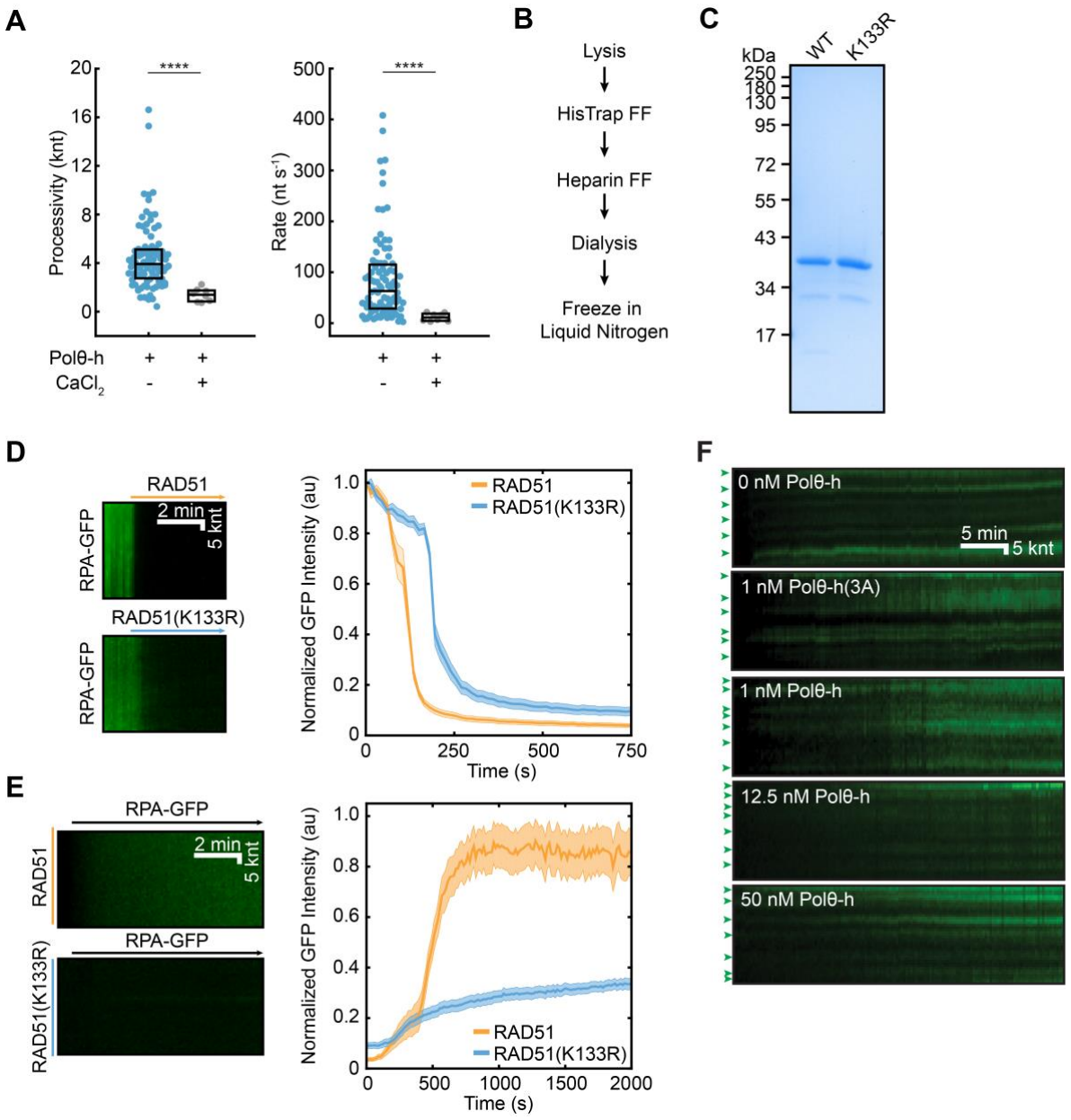

Figure S4: Characterization of RAD51(K133R) and its exchange with RPA. (A) Polθ-h is unable to remove RPA-GFP in the presence of $CaCl_2$. Boxes display the median and IQR. **(B)** Schematic of the RAD51 purification protocol. **(C)** SDS-PAGE gel of recombinant WT RAD51 and RAD51(K133R). Expected molecular weights are 37 kDa. **(D)** Kymographs of RAD51 dependent removal of RPA-GFP (left). Quantification of normalized RPA-GFP fluorescence over time (right). We analyzed 25 DNA molecules for both WT RAD51 and RAD51(K133R). **(E)** RAD51(K133R) is resistant to replacement by RPA as compared WT RAD51. Left: kymographs of RAD51 filament turnover as monitored by RPA-GFP. Right: quantification of the normalized RPA-GFP fluorescence (N=25 for both conditions). **(F)** Kymographs of RPA-GFP foci (green arrows) on RAD51(K133R) ssDNA curtains at the indicated Polθ-h concentrations.

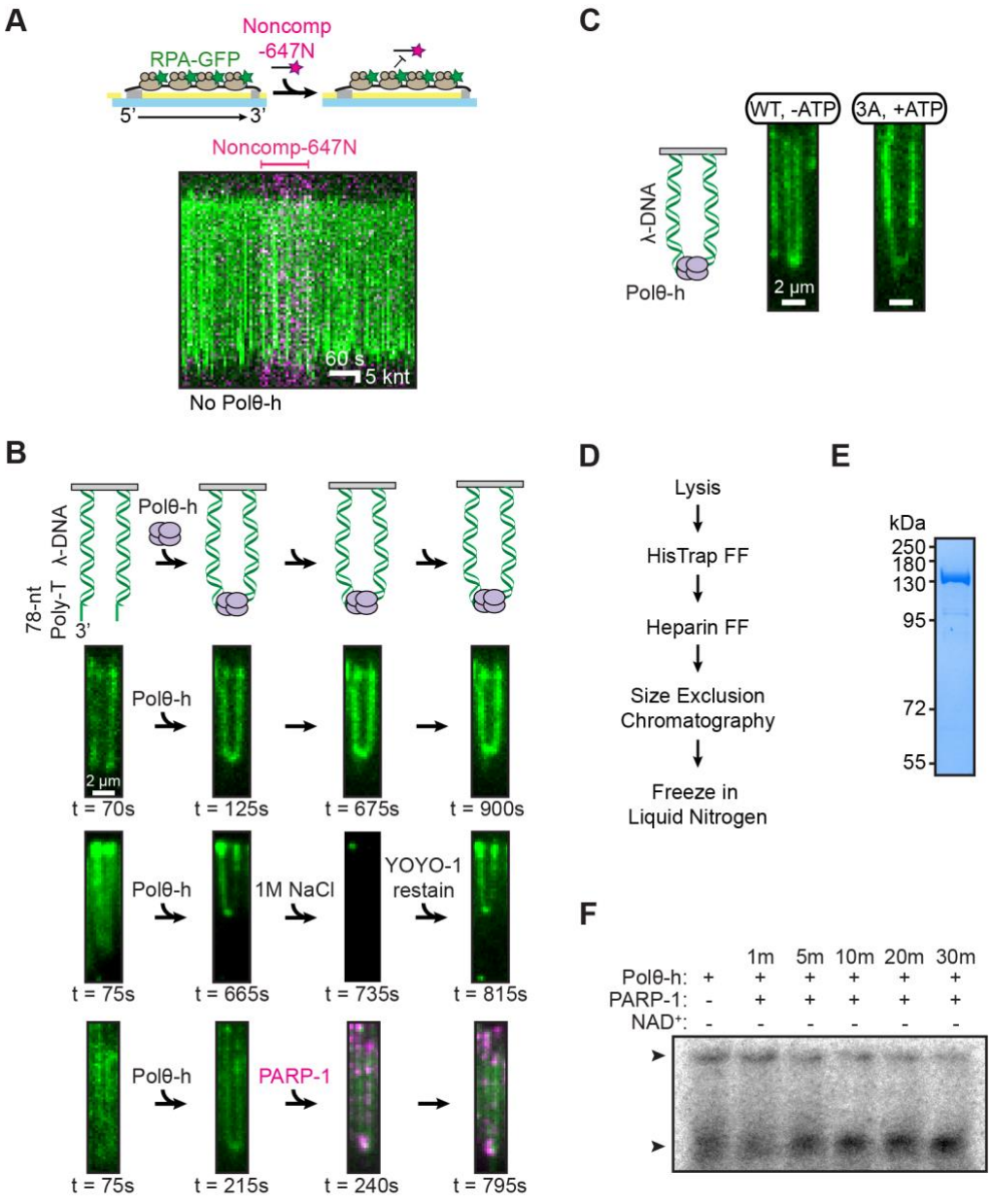

Figure S5: DNA bridging requires Polθ-h and is ATP independent. (A) Cartoon and kymograph of noncomplementary-647N (magenta) oligonucleotide injection in the absence of Polθ-h. ssDNA is bound with RPA-GFP (green). **(B)** Polθ-h tethering of two dsDNA ends persists for > 15 minutes and is resistant to 1M NaCl or the addition of PARP-1 (magenta) without NAD^+. The dsDNA substrate is visualized with the intercalating dye YOYO-1 (green). **(C)** Polθ-h tethers two ssDNA oligos annealed to a dsDNA molecule in the absence of ATP. The ATPase mutant, Polθ-h(3A), also tethered DNA. The dsDNA substrate is visualized with the intercalating dye YOYO-1 (green). **(D)** Schematic of the PARP-1 purification protocol. **(E)** SDS-PAGE gel of recombinantly purified PARP-1. N-terminal expression tags remain attached. Expected molecular weight is 129 kDa. **(F)** Prebound Polθ-h and radiolabeled ssDNA oligonucleotide were incubated with PARP-1 without NAD^+ over time.

Table S1: **Polθ-h velocity and processivity on RPA-ssDNA**

Polθ-h	Nucleotide	Processivity, knt (IQR)	Relative processivity decrease	Rate, nt s^{-1} (IQR)	Relative rate decrease	N (foci)
WT	ATP	3.9 (2.7-5.1)	-	63 (28-117)	-	91
WT	-	0.6 (0.1-1.2)	7x	4 (2-12)	16x	57
3A	ATP	0.3 (0.1-0.5)	13x	1 (0.5-4)	63x	46
-	ATP	0.4 (0.1-0.5)	10x	2 (0.2-5)	32x	55
WT	ATP / Ca^{2+}	1.4 (0.8-1.8)	3x	11 (4-20)	6x	8
SrtA-647N	ATP	0.2 (0-0.4)	20x	5 (0-10)	13x	18
Flag-647N	ATP	0.4 (-0.5-0.8)	10x	10 (0-42)	6x	20

Table S2: **Quantification of Polθ-h foci on RPA-ssDNA**

Polθ-h	Concentration, nM	Average foci per 20 pixels (S.D.)	N (ssDNA molecules)
WT	50	3.8 (0.71)	38
WT	12.5	2.7 (0.83)	36
WT	1	1.0 (0.54)	35
3A	1	0.56 (0.45)	41
-	0	0.37 (0.39)	46

Table S3: Polθ-h velocity and processivity on RAD51(K133R) filaments

Polθ-h	Nucleotide	Processivity, knt (IQR)	Relative processivity decrease	Rate, nt s^{-1} (IQR)	Relative rate decrease	N (foci)
WT	ATP	1.3 (0.5-1.9)	-	8 (3-19)	-	53
3A	ATP	0.4 (0.3-0.6)	3x	2 (0-4)	4x	41
-	ATP	0.5 (0.2-1.0)	3x	3 (1-7)	3x	36

Table S4: Quantification of Polθ-h foci on RAD51(K133R)-ssDNA

Polθ-h	Concentration (nM)	Average foci per 20 pixels (S.D.)	N (ssDNA molecules)
WT	50	3.3 (0.63)	38
WT	12.5	3.0 (0.75)	40
WT	1	2.9 (0.70)	43
3A	1	2.7 (0.43)	27
-	0	2.8 (0.41)	44

Table S5: **Oligonucleotides used in this study.**

Oligonucleotide	Sequence (5' to 3')
Template	/Phos/AG GAG AAA AAG AAA AAA AGA AAA GAA GG
Primer	/Biosg/TC TCC TCC TTC T
Comp-647N	/AT647/AGG AGA AAA AGA AAA AAA GAA AAG AAG G
Noncomp-647N	/AT647/TCC TCT TTT TCT TTT TTT CTT TTC TTC C
Poly-T_{50}	T_{50}
NJ061	GGG TTG CGG CCG CTT GGG
NJ062	CCC AAG CGG CCG CAA CCC
LAB07	/Phos/AGG TCG CCG CCC/BioTEG/
Lambda Poly-T	/Phos/GGG CGG CGA CCT T_{78}
IF724	GGA GAA TTC CGA ACT GGG AGG ACC CAG ATC TGT CAT ACG C
IF725	GCG TAT GAC AGA TCT GGG TCC TCC CAG TTC GGA ATT CTC C
IF733	CTC CTA CAA GTG CTG GGG CGA CTC TTG TGG CAG
IF734	GGA ATG GTG GTT GTG GCT GCA TTA CAT ATG CTG GGA GAC TC